

Self-consistent time-dependent harmonic approximation for the Sine-Gordon model out of equilibrium

Yuri D. van Nieuwkerk and Fabian H. L. Essler
Rudolf Peierls Centre for Theoretical Physics, Parks Road, Oxford OX1 3PU
(Dated: December 18, 2018)

We derive a self-consistent time-dependent harmonic approximation for the quantum sine-Gordon model out of equilibrium and apply the method to the dynamics of tunnel-coupled one-dimensional Bose gases. We determine the time evolution of experimentally relevant observables and in particular derive results for the probability distribution of subsystem phase fluctuations. We investigate the regime of validity of the approximation by applying it to the simpler case of a nonlinear harmonic oscillator, for which numerically exact results are available. We complement our self-consistent harmonic approximation by exact results at the free fermion point of the sine-Gordon model.

I. INTRODUCTION

The study of isolated quantum many-body systems out of equilibrium has seen a series of striking successes in the past decades, characterized by a fruitful interplay between theory and experiment. The possibility of analyzing the non-equilibrium dynamics of one-dimensional gases in particular^{1–3} stimulated a multitude of theoretical developments concerning the equilibration of observables and spreading of correlations and entanglement after quantum quenches^{4–10}. In turn, cold atom experiments have been successful in confirming many of these theoretical ideas directly^{11–16}. A particularly nice example is offered by matter-wave interferometry¹⁷ using pairs of split one-dimensional Bose gases^{13–15,18–23}, which can often be modelled theoretically using Luttinger Liquid theory^{24,25}. This approach permits a theoretical description of the dynamics of observables as well as their full quantum mechanical probability distribution functions^{26–28}, which were found to be in good correspondence with experiment^{13,15}.

Of particular interest to our work is the case when a pair of one-dimensional Bose gases is connected via a finite potential barrier^{19–22}, so that tunnelling can occur. The low-energy physics of this setup is governed by a quantum sine-Gordon model²⁹

$$\begin{aligned} H_{\text{SG}} &= H_0 - t_{\perp} \int_L dx \cos \phi(x), \\ H_0 &= \frac{v}{2\pi} \int_L dx \left[K(\partial_x \phi(x))^2 + \frac{1}{K} (\partial_x \theta(x))^2 \right]. \end{aligned} \quad (1)$$

Here the bosonic fields ϕ and $\partial_x \theta$ satisfy canonical commutation relations $[\partial_x \theta(x), \phi(y)] = i\pi\delta(x-y)$ and are compactified according to $\phi = \phi + 2\pi$ and $\theta = \theta + \pi$. The real parameters v, t_{\perp} and $K > 1/2$ are as yet undetermined, but will acquire physical meaning in what follows. Experiments have focussed on finite temperature equilibrium properties³⁰ and non-equilibrium dynamics in presence of a nonzero initial phase difference³¹ in the large- K regime. The latter experiments observed damped phase oscillations and relaxation to a phase-locked state, for which no theoretical explanation is known³². On the theoretical side there have been a number of works investigating the dynamics after quantum quenches to the sine-Gordon model. The limit $K \rightarrow \infty$ is amenable to a simple harmonic approximation^{34–37}, while at $K = 1/4$ the sine-Gordon model is equivalent to a free massive Dirac fermion and this can be used to obtain exact results^{34,35}. In Ref. 33 a combination of semiclassical and perturbative methods was used to study the rephasing dynamics for two coherently split condensates without initial phase difference. Ref. 38 investigated the time dependence of one-point functions in the repulsive regime $K < 1/4$ for quenches from an “integrable” initial state by a combination of quench action^{39,40} and linked-cluster expansion^{41,42} methods. In Ref. 43 semiclassical methods^{44,45} were applied to the same problem, while quenches from the same class of initial states to the attractive regime of the sine-Gordon model were considered in Refs 46, 48, and 49. A novel semiclassical approach was developed in Ref. 50 and used to determine the time-dependence of one and two-point functions as well as the probability distribution of the phase. The truncated conformal space approach⁴⁷ was applied in Ref. 51 to study the time evolution of two and four-point functions after a quantum quench. A very recent work⁵² addressed the phase-locking behaviour observed in the experiments³¹ by applying a combination of numerical methods to the phase dynamics in the sine-Gordon model. These findings are at variance with the experimental observations, although the parameter window of the methods does not currently extend to the relevant regime of weak interactions. This means that in spite of tentative evidence to the contrary, it is as yet unclear whether the observed relaxation to a phase-locked state is captured by a description in terms of a sine-Gordon model.

The aim of this work is to contribute to this discussion by improving on the known quadratic approximation, valid at weak interaction strengths, and replacing it by a self-consistent harmonic approximation which approximates the full cosine potential in a time-dependent manner. Such an approximation has been successfully employed for ϕ^4 -theory,

both in equilibrium⁵³ and out of equilibrium⁵⁴, and it has been formulated for the sine-Gordon model in Ref. 55. We present an alternative derivation of the method, leading to a set of coupled nonlinear equations of motion, which we solve numerically. This not only yields correlation functions, but also allows for the calculation of full distribution functions for the relevant observables. As an application of this method, we show that for squeezed initial states relevant for cold-atom experiments, the model exhibits density-phase oscillations with a time-dependent modulation of the amplitude. This amplitude modulation depends on the number-squeezing factor which characterizes the initial state. These results are complemented by exact calculations at the free fermion point of the sine-Gordon model, where strong damping of density-phase oscillations is observed.

II. DERIVATION OF THE SELF-CONSISTENT HARMONIC APPROXIMATION

Our point of departure is the quantum sine-Gordon model (1) on a ring of circumference L . We are interested in non-equilibrium dynamics after a quantum quench: the system is prepared in an initial pure state $|\psi(0)\rangle$ which is not an eigenstate of H_{SG} and which satisfies Wick's theorem. The subsequent time evolution of the system is then described by the time-dependent Schrödinger equation

$$|\psi(t)\rangle = e^{-iH_{\text{SG}}t}|\psi(0)\rangle. \quad (2)$$

The self-consistent time-dependent harmonic approximation (SCTDHA) consists of replacing the exact time evolution operator with

$$e^{-iH_{\text{SG}}t} \longrightarrow U_{\text{SCH}}(t) = T e^{-i \int_0^t H_{\text{SCH}}(\tau)d\tau}, \quad (3)$$

where

$$H_{\text{SCH}}(t) = H_0 - t_\perp \int_L dx [f(x, t) + g(x, t)\phi(x) + h(x, t)\phi^2(x)]. \quad (4)$$

The time-dependent functions in (4) are determined in a self-consistent way as follows. We assume that the Bose field can be decomposed into creation/annihilation parts with respect to the time evolved state $|\psi_{\text{SCH}}(t)\rangle = U_{\text{SCH}}(t)|\psi(0)\rangle$

$$\begin{aligned} \phi(x) &= \langle\phi(x)\rangle_t + \phi^+(t, x) + \phi^-(t, x), \\ \phi^-(t, x)|\psi_{\text{SCH}}(t)\rangle &= 0 = \langle\psi_{\text{SCH}}(t)|\phi^+(t, x), \end{aligned} \quad (5)$$

where the commutator $[\phi^+(t, x), \phi^-(t, y)]$ is a c-number and

$$\langle\phi(x)\rangle_t = \langle\psi_{\text{SCH}}(t)|\phi(x)|\psi_{\text{SCH}}(t)\rangle. \quad (6)$$

The existence of the decomposition (5) holds for the class of initial states described in Appendix A. We then define a *normal ordering* operation : ϕ^n : by stipulating that in a normal ordered expression all $\phi^-(t)$ appear on the rightmost side of any product. In particular we have

$$:\phi^n := \sum_{m=0}^n \binom{n}{m} \langle\phi\rangle_t^{n-m} : (\phi^+(t) + \phi^-(t))^m:. \quad (7)$$

Applying this normal ordering procedure to $\cos(\phi)$ we find

$$\cos(\phi(x)) = :\cos(\phi(x)) : e^{-\frac{1}{2}\langle\langle\phi^2(x)\rangle\rangle_t} = \sum_{n=0}^{\infty} \frac{(-1)^n}{(2n)!} :\phi^{2n}(x) : e^{-\frac{1}{2}\langle\langle\phi^2(x)\rangle\rangle_t}, \quad (8)$$

where $\langle\langle . \rangle\rangle$ denotes connected correlation functions

$$\langle\langle\phi^2(x)\rangle\rangle_t = \langle\phi^2(x)\rangle_t - \langle\phi(x)\rangle_t^2. \quad (9)$$

We now use (7) and neglect all higher than quadratic terms in fluctuations i.e. we set

$$:(\phi^+(t) + \phi^-(t))^m: \longrightarrow 0 \quad \forall \quad m > 2. \quad (10)$$

This results in the time-dependent Hamiltonian (4) subject to the self-consistency conditions

$$\begin{aligned} f(x, t) &= \left[\left(1 + \frac{1}{2} \langle\langle\phi^2(x)\rangle\rangle_t \right) \cos(\langle\phi(x)\rangle_t) + \langle\phi(x)\rangle_t \sin(\langle\phi(x)\rangle_t) \right] e^{-\frac{1}{2}\langle\langle\phi^2(x)\rangle\rangle_t}, \\ g(x, t) &= [\langle\phi(x)\rangle_t \cos(\langle\phi(x)\rangle_t) - \sin(\langle\phi(x)\rangle_t)] e^{-\frac{1}{2}\langle\langle\phi^2(x)\rangle\rangle_t}, \\ h(x, t) &= -\frac{1}{2} \cos(\langle\phi(x)\rangle_t) e^{-\frac{1}{2}\langle\langle\phi^2(x)\rangle\rangle_t}. \end{aligned} \quad (11)$$

A. Alternative Derivation

The SCDTHA is perhaps more naturally derived on the level of the equations of motion, as is done in Ref. 55. Since the cosine term in the Sine-Gordon Hamiltonian (1) contains all positive, even powers of the field, it generates an infinite set of coupled partial differential equations relating the time evolution of all connected n -point functions, i.e. a BBGKY-hierarchy. This hierarchy is truncated by assuming that all connected n -point functions are negligible above a certain order n . In the SCDTHA, one truncates at quadratic order, meaning all higher cumulants are set to zero. For a Gaussian initial state there will always be some time scale up to which this is a good approximation, see e.g. Refs 56 and 57. Following Ref. 55 we separate the field into its expectation value and fluctuations around it

$$\phi(x, t) = \langle \phi(x, t) \rangle + \hat{\chi}(x, t). \quad (12)$$

The equation of motion of the Bose field is then

$$\begin{aligned} (v^2 \partial_x^2 - \partial_t^2) \phi(x, t) &= \frac{v\pi t_\perp}{K} \sin(\phi(x, t)) \\ &= \frac{v\pi t_\perp}{K} [\sin(\langle \phi(x, t) \rangle) \cos(\hat{\chi}(x, t)) + \cos(\langle \phi(x, t) \rangle) \sin(\hat{\chi}(x, t))] . \end{aligned} \quad (13)$$

Assuming that all higher cumulants of the fluctuation field are negligible the right-hand side can be approximated by

$$\frac{v\pi t_\perp}{K} [\sin(\langle \phi(x, t) \rangle) : \cos(\hat{\chi}(x, t)) : + \cos(\langle \phi(x, t) \rangle) : \sin(\hat{\chi}(x, t)) :] e^{-\frac{1}{2}\langle\langle \hat{\chi}^2 \rangle\rangle}. \quad (14)$$

The equation of motion for the expectation value then becomes

$$(v^2 \partial_x^2 - \partial_t^2) \langle \phi(x, t) \rangle = \frac{v\pi t_\perp}{K} \sin(\langle \phi(x, t) \rangle) e^{-\frac{1}{2}\langle\langle \hat{\chi}^2 \rangle\rangle}. \quad (15)$$

Finally we linearize the equation of motion for the fluctuation field

$$\left[v^2 \partial_x^2 - \partial_t^2 - \frac{v\pi t_\perp}{K} \cos(\langle \phi(x, t) \rangle) e^{-\frac{1}{2}\langle\langle \hat{\chi}^2(x, t) \rangle\rangle} \right] \hat{\chi}(x, t) = 0 . \quad (16)$$

It is easy to verify that the equations of motion (15) and (16) are exactly the same as the Heisenberg equations of motion with regards to $H_{\text{SCH}}(t)$

$$\frac{\partial \phi(x, t)}{\partial t} = i U_{\text{SCH}}(t) [H_{\text{SCH}}(t), \phi(x)] U_{\text{SCH}}^\dagger(t). \quad (17)$$

B. Mode expansion

The mode expansions for the Bose field and the dual field can be cast in the form

$$\phi(x) = \sum_j u_j e^{iq_j x} (b_j - b_{-j}^\dagger) , \quad (18)$$

$$\frac{\partial_x \theta(x)}{\pi} = \frac{-i}{2u_0 L} (b_0 + b_0^\dagger) + \sum_{j \neq 0} \frac{ie^{iq_j x}}{2u_j L} (b_j + b_{-j}^\dagger) , \quad (19)$$

where $q_j = 2\pi j/L$ and we have introduced coefficients

$$u_j = \begin{cases} \left| \frac{\pi}{2q_j L K} \right|^{1/2} \text{sgn}(q_j), & \text{if } j \neq 0 , \\ \frac{i}{4} \sqrt{\frac{2v}{K}} & \text{if } j = 0 . \end{cases} \quad (20)$$

The zero momentum modes take account of the periodicity of the Bose fields $\phi(x+L) = \phi(x) + 2\pi J$ and $\theta(x+L) = \theta(x) + \pi\delta N$, where δN and J are operators with integer eigenvalues²⁴. In (18,19) we have restricted our attention to the $J = 0$ subspace and introduced creation/annihilation operators by

$$b_0 = - \left(i \sqrt{\frac{2K}{v}} \phi_0 + \frac{1}{2} \sqrt{\frac{v}{2K}} \delta N \right) , \quad (21)$$

where $[\delta N, \phi_0] = i$. By construction the free part of the Hamiltonian is diagonalized by these mode expansions

$$H_0 = \frac{\pi v(\delta N)^2}{2KL} + \sum_{j \neq 0} v|q_j| b_j^\dagger b_j. \quad (22)$$

In order to describe time evolution in the self-consistent harmonic approximation it is convenient to carry out an initial state dependent canonical transformation.

C. Gaussian initial states

To guarantee the existence of a time scale over which the SCTDHA is accurate we prepare our system in a Gaussian initial state. In the following we restrict ourselves to translationally invariant Gaussian pure states for simplicity and refer to Ref. 58 for a discussion of the general case. In terms of the bosonic creation and annihilation operators any translationally invariant Gaussian pure state can be written in the form

$$|V, \vartheta, \varphi\rangle = \exp\left(V_0 \operatorname{sech} \vartheta_0 b_0^\dagger + \frac{1}{2} \sum_k e^{i\varphi_k} \tanh \vartheta_k b_k^\dagger b_{-k}^\dagger\right) |0\rangle, \quad (23)$$

where $\vartheta_k = \vartheta_{-k}$ and $\varphi_k = \varphi_{-k}$ are real coefficients. To simplify some of the equations below we introduce

$$V_k = \delta_{k,0} V_0 \in \mathbb{C}. \quad (24)$$

The operators

$$a_k = \cosh \vartheta_k b_k - e^{i\varphi_k} \sinh \vartheta_k b_{-k}^\dagger - V_k, \quad (25)$$

annihilate the initial state

$$a_k |V, \vartheta, \varphi\rangle = 0. \quad (26)$$

The two sets of creation and annihilation operators are related by a canonical transformation

$$b_k = \cosh \vartheta_k [a_k + V_k] + e^{i\varphi_k} \sinh \vartheta_k [a_{-k}^\dagger + V_{-k}^\dagger]. \quad (27)$$

D. Equations of motion

The Hamiltonian $H_{\text{SCH}}(t)$ has a mode expansion of the form

$$H_{\text{SCH}}(t) = \sum_j \left[b_j^\dagger A_j(t) b_j + \frac{1}{2} (b_j B_j^*(t) b_{-j} + \text{h.c.}) \right] + D(t) (b_0 - b_0^\dagger) + C(t), \quad (28)$$

where the coefficients $A_j(t)$, $B_j(t)$ and $D(t)$ are functions of $g(t)$ and $h(t)$ via

$$\begin{aligned} A_j(t) &= v|p_j| - 2t_\perp L|u_j|^2 h(t), \\ B_j(t) &= v|p_0|\delta_{j,0} + 2t_\perp L|u_j|^2 h(t), \\ D(t) &= -t_\perp L u_0 g(t). \end{aligned} \quad (29)$$

In the above, we have defined $q_0 = 2\pi/vL$, and $C(t)$ is a real scalar which does not affect the equations of motion. The time evolution of b_j -operators is obtained from the Heisenberg equation of motion

$$i \frac{d}{dt} b_j(t) = U_{\text{SCH}}(t) [b_j, H_{\text{SCH}}(t)] U_{\text{SCH}}^\dagger(t). \quad (30)$$

As $H_{\text{SCH}}(t)$ couples only modes with either the same or equal but opposite index and in view of (27) the time evolved annihilation operators can be expressed as

$$b_j(t) = \delta_{j,0} R(t) + S_j(t) a_j + T_j^*(t) a_{-j}^\dagger. \quad (31)$$

The initial conditions follow from (27)

$$R(0) = V_0 \cosh \vartheta_0 + V_0^* e^{i\varphi_0} \sinh \vartheta_0, \quad S_j(0) = \cosh \vartheta_j, \quad T_j^*(0) = e^{i\varphi_j} \sinh \vartheta_j. \quad (32)$$

The time dependence of $R(t)$, $S_j(t)$ and $T_j(t)$ is obtained by substituting (31) in to (30), which gives a system of coupled, first order differential equations

$$\begin{aligned} i\dot{R}(t) &= A_0(t)R(t) + B_0(t)R^*(t) - D(t), \\ i\dot{S}_j(t) &= A_j(t)S_j(t) + B_j(t)T_{-j}(t), \\ -i\dot{T}_j(t) &= A_j^*(t)T_j(t) + B_j^*(t)S_{-j}(t). \end{aligned} \quad (33)$$

We stress that Eqns (33) are *non-linear* as A , B and D are functions of R , S and T by virtue of the self-consistency conditions (11). The time evolved Bose fields in our SCTDHA are given by

$$\phi(x, t) = -2|u_0|\text{Im}(R(t)) + \sum_j u_j e^{iq_j x} \left(Q_j(t)a_j - Q_{-j}^*(t)a_{-j}^\dagger \right), \quad (34)$$

where we have defined

$$Q_j(t) = S_j(t) - T_{-j}(t), \quad \bar{Q}_j(t) = S_j(t) + T_{-j}(t). \quad (35)$$

Using that $a_j |V, \vartheta, \varphi\rangle = 0$ it is then straightforward to obtain equal-time correlation functions of the Bose field

$$\langle \phi(x, t) \rangle = -2|u_0|\text{Im}(R(t)), \quad (36)$$

$$\langle \phi(x, t)\phi(y, t) \rangle_{\text{conn}} = \sum_j |u_j|^2 |Q_j(t)|^2 \cos(q_j(x - y)). \quad (37)$$

These expectation values determine the functions $g(t)$, $h(t)$ and by (29) the parameters $A_j(t)$, $B_j(t)$, $D_j(t)$. Substituting back into (33) we arrive at a closed system of differential equations for $R_j(t)$, $S_j(t)$ and $T_j(t)$. We solve this nonlinear system numerically to obtain the full time evolution of local operators in our SCTDHA.

E. Full distribution functions and multipoint correlation functions

A nice feature of the SCTDHA is that it makes it possible to analyze not only expectation values of local operators, but the full quantum mechanical probability distributions of observables on subsystems. This is of considerable experimental and theoretical interest^{26,30,59–74}. An example relevant to realizations of the sine-Gordon model in split one-dimensional Bose gases are the probability distributions for the real and imaginary parts of the operator^{26–28}

$$\hat{\mathcal{O}}_\ell = \int_{-\ell/2}^{\ell/2} dx e^{i\hat{\phi}(x)}. \quad (38)$$

It is convenient to define a joint probability distribution of the commuting operators $\text{Re}(\hat{\mathcal{O}}_\ell)$ and $\text{Im}(\hat{\mathcal{O}}_\ell)$

$$F_\ell(t, a, b) = \langle \psi_{\text{SCH}}(t) | \delta(\text{Re}(\hat{\mathcal{O}}_\ell) - a) \delta(\text{Im}(\hat{\mathcal{O}}_\ell) - b) | \psi_{\text{SCH}}(t) \rangle. \quad (39)$$

As shown in Appendix B it is possible to obtain a multiple integral representation for this quantity in the framework of the SCTDHA

$$\begin{aligned} F_\ell(t, a, b) &= \int_{-\infty}^{\infty} \prod_j \left[d\alpha_j d\beta_j \frac{e^{-\frac{1}{2}|Q_j(t)|^{-2}(\alpha_j^2 + \beta_j^2)}}{2\pi |Q_j(t)|^2} \right] \delta \left(a - \int_{-\ell/2}^{\ell/2} dx \cos(\Phi(x, t, \boldsymbol{\alpha}, \boldsymbol{\beta})) \right) \\ &\quad \times \delta \left(b - \int_{-\ell/2}^{\ell/2} dx \sin(\Phi(x, t, \boldsymbol{\alpha}, \boldsymbol{\beta})) \right), \end{aligned} \quad (40)$$

where

$$\Phi(x, t, \boldsymbol{\alpha}, \boldsymbol{\beta}) = \langle \phi(0, t) \rangle - \sum_j |u_j| \left(\alpha_j \cos(p_j x) + \beta_j \sin(p_j x) \right). \quad (41)$$

We see that the distribution function is determined by the expectation value $\langle \phi(0, t) \rangle$, set by $R(t)$ via (36), along with quadratic fluctuations α_j and β_j , determined by the covariance matrix $|Q_j(t)|^2$. The essential quantities $R(t)$ and $Q(t)$ are obtained by solving the nonlinear, self-consistent system of equations (33). The distribution function (40) can be conveniently sampled using Monte Carlo techniques: one draws numbers α_j and β_j from a Gaussian distribution with covariance matrix $|Q_j(t)|^2$ and computes the corresponding values of $\int_{-\ell/2}^{\ell/2} dx \exp(i\Phi(x, t, \boldsymbol{\alpha}, \boldsymbol{\beta}))$. Placing real and imaginary parts of these values in a two-dimensional histogram and normalizing the result yields $F_\ell(t, a, b)$. As a corollary of the derivation in Appendix B, we also obtain multi-point correlation functions of the vertex operator $e^{i\sigma\phi(x)}$, e.g.

$$\left\langle e^{i\sigma\phi(x, t)} e^{i\tau\phi(0, t)} \right\rangle = e^{i(\sigma+\tau)\langle\phi(0, t)\rangle} e^{-\frac{1}{2}\sum_j |u_j|^2 |Q_j(t)|^2 (\sigma^2 + \tau^2 + 2\sigma\tau \cos(q_j x))}. \quad (42)$$

III. SELF-CONSISTENT HARMONIC APPROXIMATION IN EQUILIBRIUM

If we choose self-consistent normal ordering with respect to the ground state rather than some time evolved initial state our approximation reduces to the usual self-consistent harmonic approximation for the sine-Gordon model⁷⁵. In the linear response regime at zero temperature many exact results are available for the sine-Gordon model, see e.g. Ref. 76, and it is instructive to use these to benchmark the SCHA. The exact breather mass of the sine-Gordon model is⁷⁷

$$\Delta_1 = 2 \sin\left(\frac{\pi\chi}{2}\right) \frac{2}{\sqrt{\pi}} \frac{v}{\xi} \frac{\Gamma(\chi/2)}{\Gamma((1+\chi)/2)} \left[\frac{\pi}{2} \frac{\xi^2}{v} t_\perp \frac{\Gamma(\frac{1}{1+\chi})}{\Gamma(\frac{\chi}{1+\chi})} \right]^{(1+\chi)/2}, \quad (43)$$

where $\chi = 1/(8K - 1)$ and the length scale ξ corresponds to a cutoff in momentum space at $k_c = 2\pi/\xi$.

Normal ordering with regards to the (self-consistent) ground state results in a time-independent Hamiltonian of the same structure as $H_{\text{SCH}}(t)$ in (28) and (29)), but with time-independent parameters

$$g = 0, \quad h = -\frac{1}{2} e^{-\frac{1}{2}\langle\phi^2\rangle}. \quad (44)$$

This Hamiltonian can be diagonalized by a Bogoliubov transformation of the b -operators

$$\begin{aligned} b_j &= \cosh(\gamma_j) c_j + \sinh(\gamma_j) c_{-j}^\dagger, \\ e^{-2\gamma_j} &= \frac{\pi}{2KL|u_j|^2} [(vq_j)^2 + \Delta^2]^{-\frac{1}{2}}, \end{aligned} \quad (45)$$

where we have defined

$$\Delta^2 = -2h \frac{\pi v t_\perp}{K}. \quad (46)$$

In terms of the Bogoliubov bosons we have

$$H_{\text{SCH}} = \sum_j \left[\sqrt{(vq_j)^2 + \Delta^2} c_j^\dagger c_j \right] + \tilde{C}. \quad (47)$$

The ground state of H_{SCH} the vacuum state of the c -bosons $c_j|0\rangle = 0$. The self-consistency condition for h is then obtained by calculating $\langle\phi^2\rangle = \langle 0|\phi^2(x)|0\rangle$

$$\langle\phi^2\rangle = \frac{\pi v}{2KL} \sum_j \frac{1}{\sqrt{v^2 q_j^2 + \frac{\pi v t_\perp}{K} e^{-\frac{1}{2}\langle\phi^2\rangle}}}. \quad (48)$$

A simple quadratic (*non* self-consistent) approximation of $H_{\text{SG}}(t)$ ^{36,37} would be given by $g = 0$ and $h = -1/2$, so that

$$\Delta_{\text{qdr}}^2 = \frac{\pi v t_\perp}{K}. \quad (49)$$

In Fig. 1, we present a comparison between the gap of the first breather in the sine-Gordon model (solid lines), the gap in the completely quadratic model (dotted lines) and the gap in the SCHA (dashed line). This is the appropriate comparison to make because in the K regime of interest the first breather has the smallest excitation gap over the ground state. For large enough values of K , both the SCHA and the fully quadratic model provide accurate approximations. For smaller values of K , however, the self-consistent approximation clearly offers a much better prediction of Δ than the simple harmonic approximation does. Close to the Luther-Emery point, which lies at $K = 1/4$ in our conventions, the predictions from the SCHA become poor as well.

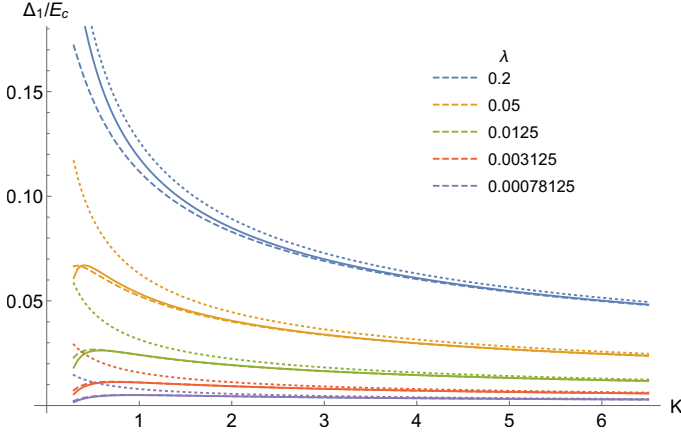


FIG. 1. Comparison between the mass gap for the fully quadratic model with $h = -1/2$ (dotted), the SCHA (dashed) and the exact result for the sine-Gordon Hamiltonian (solid curves), for several values of the dimensionless coupling $\lambda = \xi^2 t_\perp/v$. The gaps are plotted via their ratio with the cutoff energy scale, $E_c = 2\pi v/\xi$.

IV. REALIZATION BY TUNNEL-COUPLED BOSE GASES

A very interesting experimental realization of the sine-Gordon Hamiltonian (1) arises by tunnel-coupling a pair of one-dimensional Bose gases^{29,30} $H = H_{\text{LL}} + H_{\text{tunn}}$ with

$$H_{\text{LL}} = \sum_{j=1,2} \int dx \left[\frac{1}{2m} \partial_x \psi_j^\dagger \partial_x \psi_j + g \psi_j^\dagger \psi_j^\dagger \psi_j \psi_j \right], \quad (50)$$

$$H_{\text{tunn}} = -T_\perp \int dx (\psi_1^\dagger \psi_2 + \psi_2^\dagger \psi_1). \quad (51)$$

Here ψ_j are complex Bose fields with commutation relations $[\psi_i(x), \psi_j^\dagger(x')] = \delta_{i,j} \delta(x-x')$. At low energies the model (50), (51) can be bosonized using²⁴

$$\psi_j \sim \sqrt{\rho_0 + \partial_x \theta_j(x)/\pi} e^{i\phi_j(x)}, \quad (52)$$

where ϕ_j are real Bose fields, θ_j the associated dual fields and ρ_0 the average density of bosons. Expressing the resulting Hamiltonian in terms of symmetric and antisymmetric combinations $\phi = \phi_1 \pm \phi_2$, $\theta = (\theta_1 \pm \theta_2)/2$ gives a decoupled theory of a free compact Boson and a sine-Gordon model

$$\mathcal{H} = \sum_{j=s,a} \frac{v}{2\pi} \int dx \left[K(\partial_x \phi_j(x))^2 + \frac{1}{K} (\partial_x \theta_j(x))^2 \right] - t_\perp \int dx \cos \hat{\phi}_a(x). \quad (53)$$

The (less relevant) coupling between the two sectors will be analyzed in a forthcoming publication⁵⁸. Importantly the symmetric sector only gives negligible contributions to the experimentally relevant observables in the large- K regime⁷¹. The cutoff for the low-energy description (53) is given by the healing length of the gas $\xi = \pi/mv$ and $t_\perp = 2\rho_0 T_\perp$. For weak interactions, the effective parameters v and K can be related^{29,78} to the parameters in the microscopic model (50) by

$$v = \frac{\rho_0}{m} \sqrt{\gamma} \left(1 - \frac{\sqrt{\gamma}}{2\pi} \right)^{1/2}, \quad K = \frac{\pi}{2\sqrt{\gamma}} \left(1 - \frac{\sqrt{\gamma}}{2\pi} \right)^{-1/2}.$$

Here $\gamma = mg/\rho_0$ is the dimensionless interaction parameter. For later convenience we define a dimensionless coupling constant for the cosine term by

$$\lambda = \frac{\xi^2 t_\perp}{v}. \quad (54)$$

In the experiments by the Vienna group an initial state is prepared by splitting of a single one-dimensional condensate into two³¹, which can be modelled by an initial condition^{27,28}

$$\left\langle \frac{\partial_x \hat{\theta}(x)}{\pi} \frac{\partial_y \hat{\theta}(y)}{\pi} \right\rangle_c = \eta \frac{\rho}{2} \delta_\xi(x-y). \quad (55)$$

Here δ_ξ denotes a delta function which is smeared over the healing length of the gas. In terms of the squeezed coherent state (23), this initial condition is obtained²⁸ by choosing Bogoliubov angles $\varphi_j = 0$ and

$$e^{-2\vartheta_j} = \begin{cases} \frac{|q_j|K}{\pi\eta\rho}, & \text{if } j \neq 0, \\ \frac{4K}{vL\eta\rho}, & \text{if } j = 0. \end{cases} \quad (56)$$

The parameter η tunes the number and phase fluctuations in the initial state.

1. Choice of parameters

To enable a comparison of the results presented below with experimental observations we will from here on fix the parameters defining our model (53) following Ref. 23: the one-dimensional density is taken to be $\rho_0 = 45 \mu\text{m}^{-1}$, the healing length $\xi = \hbar\pi/mv = \pi \times 0.42 \mu\text{m}$ and longitudinal size $L = 160\xi$. Note that the latter is a factor 2 larger than the length reported in 23. We have made this adjustment to be able to follow the dynamics over longer timescales, before boundary effects come into play. For the case of ^{87}Rb atoms, the above amounts to $L \approx 212 \mu\text{m}$, with a sound velocity given by $v \approx 1.738 \cdot 10^{-3} \text{ m/s}$ and a Luttinger parameter of $K \approx 28$, in our conventions.

A. Time-evolution of the zero mode

As we are focussing on translational invariant situations in this work the zero momentum modes of the Bose fields play a key role. In the full Hamiltonian (28) the zero momentum modes are sensitive to the dynamics of the finite momentum modes by virtue of the self-consistency conditions. It is instructive to ignore such effects and consider the SCTDHA for a toy model that involves only the zero mode

$$H_J = \frac{\pi v}{2KL} \delta \hat{N}^2 - t_\perp L \cos(\hat{\phi}_0), \quad (57)$$

where $[\delta \hat{N}, \hat{\phi}_0] = i$ and we have retained the various parameters from the full model. As (57) involves only a single degree of freedom it is straightforward to obtain exact results by numerically integrating the corresponding Schrödinger equation. This allows us to benchmark the SCTDHA. As initial state we choose a squeezed state $|\chi(0)\rangle$ with wave function in the ϕ -representation

$$\chi(\phi) = \left(\frac{1}{2\pi\sigma^2} \right)^{1/4} e^{-\frac{(\phi-\Phi_0)^2}{4\sigma^2}} e^{-i\delta N_0 \phi}, \quad (58)$$

where $\sigma^2 = 1/(2\eta\rho L)$ and Φ_0 , δN_0 are free parameters. In the SCTDHA the Hamiltonian (57) is replaced by

$$H'_J = \frac{\pi v}{2KL} \delta \hat{N}^2 - t_\perp L \left(f(t) + g(t)\hat{\phi}_0 + h(t)\hat{\phi}_0^2 \right). \quad (59)$$

The self-consistency conditions for f , g and h are obtained from (11) by replacing $\phi(x) \rightarrow \hat{\phi}_0$. For reference, we also consider time evolution with a simple harmonic Hamiltonian obtained from (57) by expanding the cosine to second order in $\hat{\phi}_0$

$$H_{HO} = \frac{\pi v}{2KL} \delta \hat{N}^2 + \frac{t_\perp L}{2} \hat{\phi}_0^2, \quad (60)$$

The ground state wave function of H_{HO} is given by (58) with $\Phi_0 = 0 = \delta N_0$ and $\eta_0 \equiv \rho^{-1} \sqrt{t_\perp K/v\pi}$.

In Fig. 2 and Appendix C we compare time evolution under the Hamiltonians H_J (green line), H_{HO} (red, dotted line), and H'_J (blue line), with $\Phi_0 = 0.1$ and two choices of initial state $|\chi(0)\rangle$. We observe fast oscillations of $\langle \hat{\phi}_0 \rangle \equiv \langle \chi(t) | \hat{\phi}_0 | \chi(t) \rangle$ in time with a slowly varying envelope. This envelope shrinks (Fig. 2) or expands (Appendix C), depending on the initial values Φ_0 and δN_0 . We observe that the amplitude modulation is more pronounced when η/η_0 is either large or small, which corresponds to initial states with either large phase or number fluctuations. Such states are sensitive to the anharmonicity of the cosine potential and their time evolution will exhibit larger deviations from that of a simple harmonic oscillator. We see that the SCTDHA is significantly better than the simple harmonic approximation H_{HO} . The SCTDHA neglects higher connected correlations and is accurate as long as the latter are

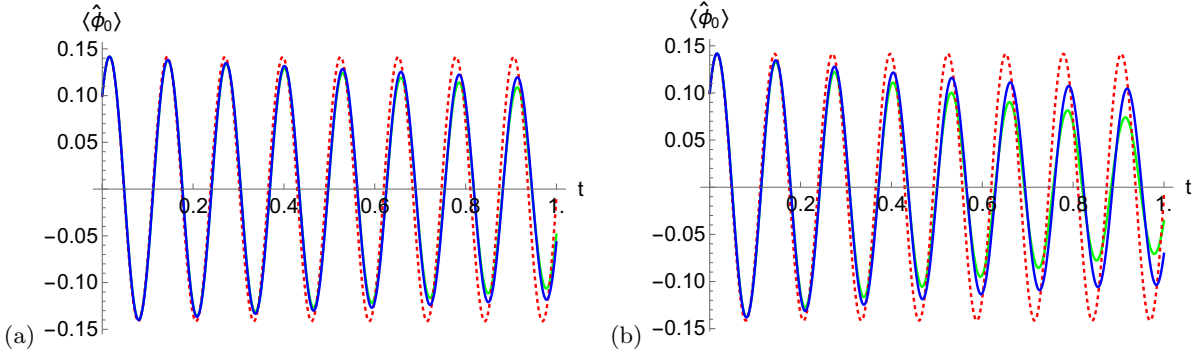


FIG. 2. Time-evolution of $\langle \hat{\phi}_0 \rangle$ under the full Hamiltonian H_J (green line), the quadratic approximation H_{HO} (red dots) and the self-consistent harmonic approximation H'_J (blue line). The parameters are $\lambda = 0.12$ and (a) $\eta = 4\eta_0$; (b) $\eta = 8\eta_0$.

small. The contribution of the connected correlation functions to the expectation values of $\hat{\phi}_0^3$ and $\hat{\phi}_0^4$ are respectively

$$\langle \hat{\phi}_0^3 \rangle = \langle \hat{\phi}_0^3 \rangle_c + 3 \langle \hat{\phi}_0^2 \rangle_c \langle \hat{\phi}_0 \rangle + \langle \hat{\phi}_0 \rangle^3, \quad (61)$$

$$\langle \hat{\phi}_0^4 \rangle = \langle \hat{\phi}_0^4 \rangle_c + 4 \langle \hat{\phi}_0^3 \rangle_c \langle \hat{\phi}_0 \rangle + 3 \langle \hat{\phi}_0^2 \rangle_c^2 + 6 \langle \hat{\phi}_0^2 \rangle_c \langle \hat{\phi}_0 \rangle^2 + \langle \hat{\phi}_0 \rangle^4, \quad (62)$$

Figs 3 and 4 show the time evolution of the neglected connected contributions and compare them to the full expectation value. By our choice of initial state the cumulants are initially zero and then grow in time. The growth of even

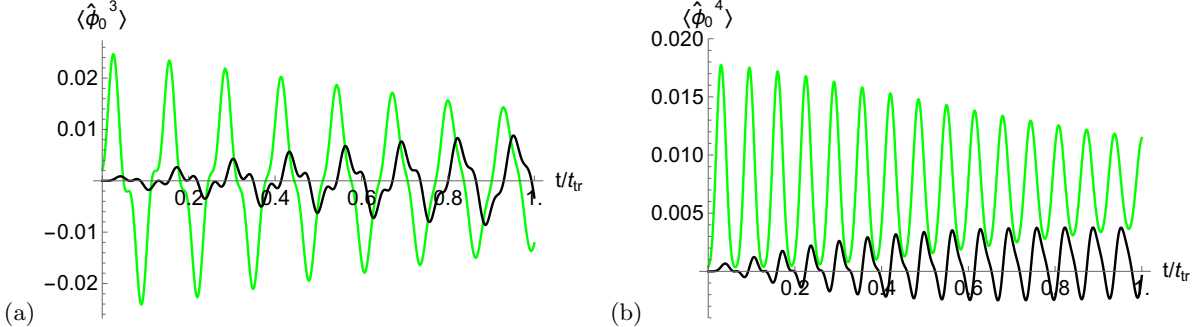


FIG. 3. Time-evolution of higher moments under the full cosine potential (green lines) compared to the contributions of the higher cumulants $\langle \hat{\phi}_0^3 \rangle_c$ and $\langle \hat{\phi}_0^4 \rangle_c$ (black lines). The parameters are $\lambda = 0.12$, $\eta = 4\eta_0$, $K = 1$, with the remaining ones chosen as described in IV 1.

cumulants is inhibited by choosing the squeezing parameter η close to η_0 , whereas odd cumulants are inhibited by choosing Φ_0 and δN_0 close to 0. In our examples the cumulants remain small and concomitantly the SCTDHA is a good approximation.

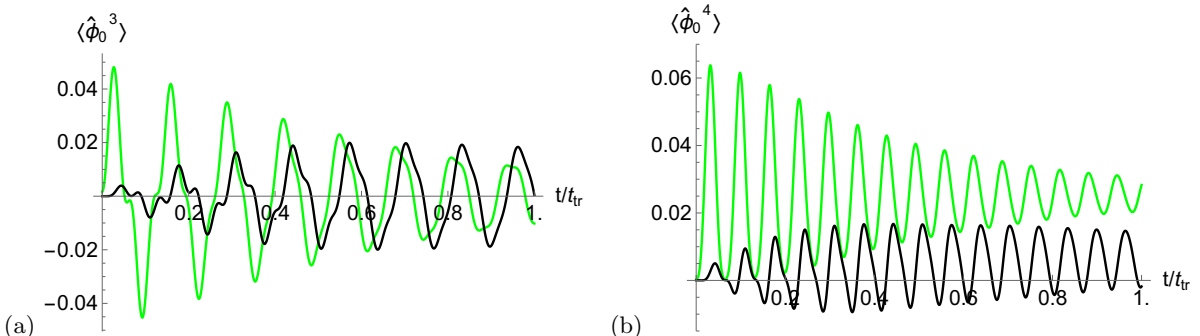


FIG. 4. The same as Fig. 3, but with squeezing parameter $\eta = 8\eta_0$.

B. Time-evolution in the SCTDHA for the sine-Gordon model

Having tested the self-consistent harmonic approximation in the controlled setting of single-body quantum mechanics, we now apply it to the sine-Gordon field theory, using the formalism developed in section II. Motivated by experiment we focus on the following observables:

- The one-point functions of density $\langle \partial_x \theta(x, t) \rangle$ and phase $\langle \phi(x, t) \rangle$. As we are restricting ourselves to translationally invariant situations these are x -independent.
- The full quantum mechanical probability distribution of $\int_{-\ell/2}^{\ell/2} dx \sin(\phi(x))$

$$P_\ell(t, \mu) = \langle \psi_{\text{SCH}}(t) | \delta\left(\mu - \int_{-\ell/2}^{\ell/2} dx \sin(\phi(x))\right) | \psi_{\text{SCH}}(t) \rangle. \quad (63)$$

If Fig. 5 we show parametric plots for the time dependence of the average density and phase in the SCTDHA for two different choices of parameters. In a purely harmonic theory the resulting trajectory would be closed, *cf.* the green line in Fig. 5(b).

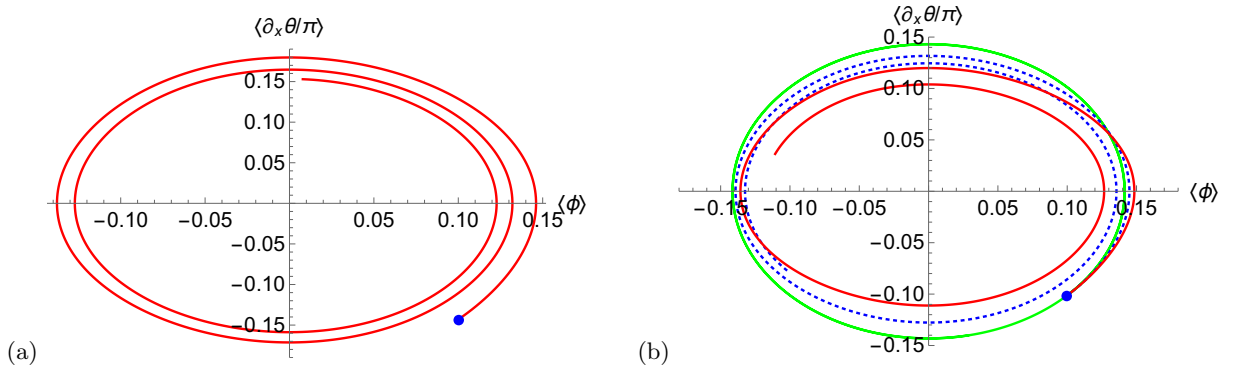


FIG. 5. (a) Density-phase oscillations in the SCTDHA. The parameters are as described in IV 1 and $\lambda = 0.4$, $\eta = 1$. A modulation of the amplitude can be observed, which is not present in a simple approximation. (b) Same as (a) but with $\lambda = 0.2$, $\eta = 0.5$ (blue) and $\eta = 1$ (red). For comparison we also show the result of a simple harmonic approximation (green line). The modulation is seen to increase with η .

In contrast the amplitude of these oscillations gets modulated in time in the SCTDHA. We observe that these modulations become more pronounced as the squeezing parameter η is increased from its ground state value.

We now turn to the probability distribution function $P_\ell(t, \mu)$. In recent experiments³¹ it was observed that the variance of the probability distribution of the phase exhibits a rapid narrowing. A detailed explanation why these experiments have access to the probability distribution of the phase itself is given in Ref. 71. An important question is whether such behaviour arises in the framework of the sine-Gordon model. In Figs 6 and 7 we show results for $P_\ell(t, \mu)$ for two integration lengths ℓ obtained in the SCTDHA and a simple harmonic approximation. Both display oscillatory behaviour in time and no narrowing of the variance is observed. In fact, the variance in the SCTDHA is slightly larger than the simple harmonic result. Comparing Fig. 6 to 7 we observe that increasing the integration length leads to a narrowing of $P_\ell(t, \mu)$.

V. DYNAMICS AT THE LUTHER-EMERY (LE) POINT

The SCTDHA is expected to work best at large values of the Luttinger parameter K . It is instructive to complement the large- K results presented above by exact results at the free fermion point of the sine-Gordon model. In our conventions the LE point occurs at $K = 1/4$. Quench dynamics at the LE point has been previously considered in Ref. 34 and 35 but that analysis did not cover the class of initial states of interest to us here. Two remarks are in order before we proceed:

- The LE point occurs at an unphysical value of K as far as the realization of the sine-Gordon model in the context of tunnel-coupled Bose gases is concerned. In that context the Luttinger parameter runs from $K = 1/2$ (hard-core repulsion) to $K \rightarrow \infty$ (non-interacting bosons).

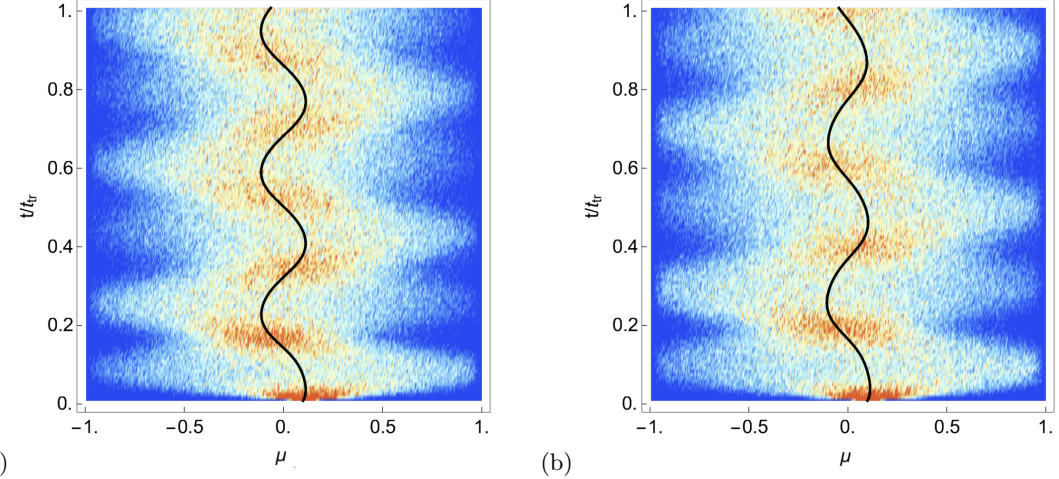


FIG. 6. (a) Probability distribution function $P_\ell(t, \mu)$ for a very short integration length $\ell = \xi$ in a simple harmonic approximation to the sine-Gordon model corresponding to $g = 0$ and $h = -1/2$ in (11). Parameters are as described in IV 1 and $\lambda = 0.2$. The black line shows the average of the PDF. (b) Same as (a) but computed in the SCTDHA.

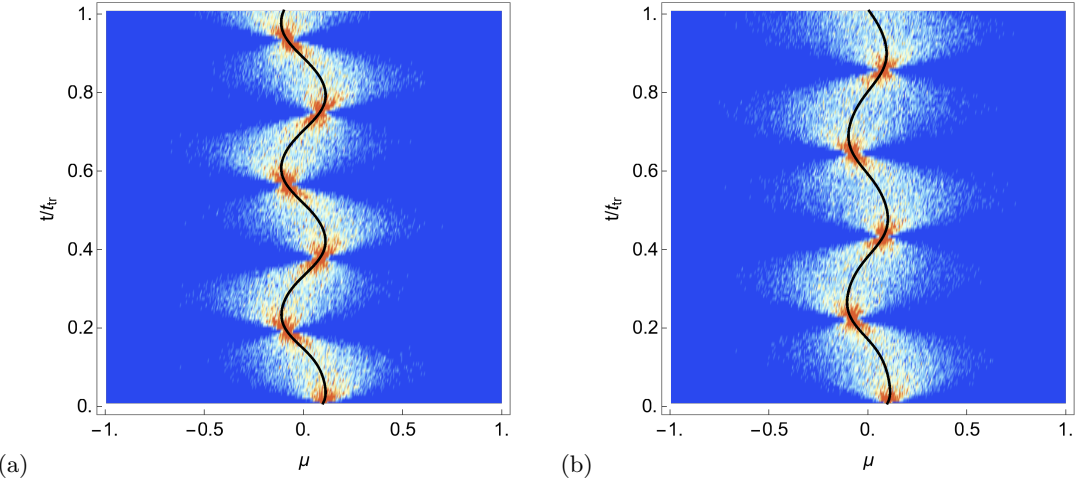


FIG. 7. Same as Fig. 6 but with a long integration length $\ell = L$.

- The SCTDHA is not expected to be a good approximation at the LE point. We have already seen an example of this in section III. The fundamental problem is that the relevant degrees of freedom at the LE point are solitons and antisolitons and these are not captured by a harmonic approximation. In light of this we will refrain from attempting to apply the SCTDHA to the sine-Gordon model at $K = 1/4$.

A. Mapping to free fermions

The sine-Gordon model can be fermionized using the bosonization identities

$$R(x) = \frac{F}{\sqrt{2\pi\xi}} e^{-i\sqrt{4\pi}\varphi_R(x)}, \quad L(x) = \frac{\bar{F}}{\sqrt{2\pi\xi}} e^{i\sqrt{4\pi}\varphi_L(x)}, \quad (64)$$

where $F = \sigma_x$, $\bar{F} = \sigma_y$ are Klein factors and $\varphi_{R/L}(x)$ are chiral Bose fields defined as

$$\varphi_{R/L} = \sqrt{\frac{K}{4\pi}}\phi \pm \frac{1}{\sqrt{4\pi K}}\theta. \quad (65)$$

The fields defined in (64) fulfil anticommutation relations $\{R^\dagger(x), R(y)\} = \{L^\dagger(x), L(y)\} = \delta(x - y)$. Expectation values are always taken with respect to the vector $(1, 0)$ in Klein space. At the LE point the sine-Gordon Hamiltonian

(1) is equivalent to

$$H_F = \int_L dx [iv(L^\dagger(x)\partial_x L(x) - R^\dagger(x)\partial_x R(x)) + i\mu(R^\dagger(x)L(x) - L^\dagger(x)R(x))], \quad (66)$$

where $\mu = \pi\xi t_\perp$. Then Fermi fields have mode expansions

$$R(x) = \frac{1}{\sqrt{L}} \sum_k e^{ikx} a_k, \quad L(x) = \frac{1}{\sqrt{L}} \sum_k e^{ikx} b_k. \quad (67)$$

B. Time-evolution of density and phase

The solution to the equations of motion for the modes is

$$\begin{pmatrix} a_k(t) \\ b_k(t) \end{pmatrix} = \begin{pmatrix} \cos(\omega_k t) - i \sin(\omega_k t) \cos(2\gamma_k) & \sin(\omega_k t) \sin(2\gamma_k) \\ -\sin(\omega_k t) \sin(2\gamma_k) & \cos(\omega_k t) + i \sin(\omega_k t) \cos(2\gamma_k) \end{pmatrix} \begin{pmatrix} a_k \\ b_k \end{pmatrix}, \quad (68)$$

where

$$\sin(2\gamma_k) = \frac{\mu}{\omega_k}, \quad \cos(2\gamma_k) = \frac{vk}{\omega_k}, \quad \omega_k = \text{sgn}(k) \sqrt{(vk)^2 + \mu^2}. \quad (69)$$

Our aim is to determine the expectation values of

$$\begin{aligned} \sin(\phi(x, t)) &= -\pi\xi [R^\dagger(x, t)L(x, t) + \text{h.c.}], \\ \frac{\partial_x \theta(x, t)}{\pi} &= \frac{1}{2} [:L^\dagger(x, t)L(x, t): - :R^\dagger(x, t)R(x, t):]. \end{aligned} \quad (70)$$

Here products of operators at the same point are defined by means of a point-splitting prescription

$$:L^\dagger(x)L(x): \equiv \lim_{\epsilon \rightarrow 0} [L^\dagger(x-\epsilon)L(x+\epsilon) - \langle L^\dagger(x-\epsilon)L(x+\epsilon) \rangle_0], \quad (71)$$

where $\langle \dots \rangle_0$ denotes the expectation value with respect to the initial state under consideration. In order to make some contact with our previous discussion we choose the initial state to be $|V, \varphi, \vartheta\rangle$ in (23), i.e.

$$\langle \mathcal{O} \rangle_0 \equiv \langle V, \varphi, \vartheta | \mathcal{O} | V, \varphi, \vartheta \rangle. \quad (72)$$

The required expectation values are calculated by noting that as a consequence of translational invariance

$$\begin{aligned} \langle a_k^\dagger a_p \rangle &= \delta_{p,k} \int_L dx e^{ikx} \langle R^\dagger(x)R(0) \rangle_0, \\ \langle b_k^\dagger b_p \rangle &= \delta_{p,k} \int_L dx e^{ikx} \langle L^\dagger(x)L(0) \rangle_0, \\ \langle a_k^\dagger b_p \rangle &= \delta_{p,k} \int_L dx e^{ikx} \langle R^\dagger(x)L(0) \rangle_0. \end{aligned} \quad (73)$$

The two-point functions of Fermi fields can then be calculated using the bosonization identities (65) and (64). Specializing to initial states with initial condition $\langle \partial_x \theta(x) \rangle_0 = 0$, we find after some calculations

$$\begin{aligned} \frac{1}{\pi} \langle \partial_x \theta(x, t) \rangle_0 &= -\frac{1}{L} \sum_k \frac{2\mu}{\omega_k} \sin(\omega_k t) \cos(\omega_k t) \operatorname{Re} \langle a_k^\dagger b_k \rangle, \\ \langle \sin \phi(x, t) \rangle_0 &= \frac{1}{L} \sum_k 2\pi\xi \operatorname{Re} \left[\langle a_k^\dagger b_k \rangle^* \frac{\mu^2}{\omega_k^2} \sin^2(\omega_k t) - \langle a_k^\dagger b_k \rangle \left(\cos(\omega_k t) + i \frac{vk}{\omega_k} \sin(\omega_k t) \right)^2 \right]. \end{aligned} \quad (74)$$

These expectation values are plotted in Fig. 8, for the parameters in (IV 1), with $K = 1/4$. A strong damping of the density-phase oscillation is observed, showing that the amplitude modulations encountered in Section IV B also exist in the exact solution at the Luther-Emery point.

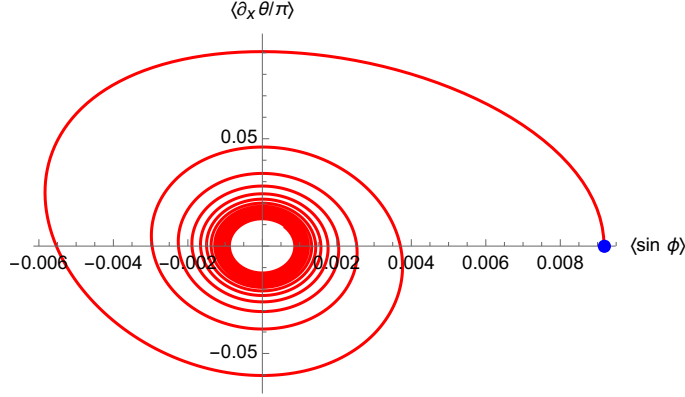


FIG. 8. Strongly damped density-phase oscillation at the Luther-Emery point. Apart from taking $K = 1/4$, we have used the parameters as reported in (IV 1), with the dimensionless coupling constant (54) set to $\lambda = 0.25$. The initial conditions are obtained from Eqs. (23) and (56) using the bosonization identity (64), with $\langle \delta N \rangle = 0$ and $\langle \phi_0 \rangle = 0.1$ at $t = 0$. Due to the enhanced phase fluctuations at the Luther-Emery point for the state under consideration, the expectation value of the sine is reduced to $\langle \sin \phi \rangle \approx 0.009$, at $t = 0$.

VI. CONCLUSIONS

We have implemented a self-consistent time-dependent approximation for the quantum sine-Gordon model out of equilibrium. The approximation incorporates anharmonic effects of the cosine potential in a time-dependent manner by reducing higher-order fluctuations of the phase field to time-dependent mean field coefficients in the Hamiltonian. This leads to a time-dependent non-interacting Hamiltonian that can be analyzed by standard methods. Its simple structure allows for the calculation of multi-point correlation functions and full quantum mechanical probability distribution functions of some observables out of equilibrium.

As an application, we have considered tunnel-coupled, coherently split Bose-gases with an initial density- and phase offset. We found that expectation values of the density and phase exhibit oscillatory behaviour with amplitudes that are modulated in time. Such modulations are not observed in a simple harmonic approximation and arise from the anharmonicity of the cosine potential. An exact calculation at the free fermion point of the sine-Gordon model also shows such modulations. These findings are of interest in relation to recent experiments by the Vienna group³¹, where qualitatively similar behaviour was observed. However, the SCTDHA does not provide a quantitative explanation of the experimental findings. Moreover, the experiments show a rapid narrowing of the probability distribution of the phase, in contrast to what we find in the SCTDHA. Our results are in accord with recent numerical studies⁵² and suggest that a simple sine-Gordon model is insufficient for describing the experiments.

Our method is very general and can in particular be applied to inhomogeneous situations. In a forthcoming publication we use it to analyze interactions between the symmetric and antisymmetric sectors in tunnel-coupled Bose gases and consider situations that are not translationally invariant⁵⁸.

ACKNOWLEDGMENTS

We are grateful to Jörg Schmiedmayer and Marine Pigneur for stimulating discussions and to the Erwin Schrödinger International Institute for Mathematics and Physics for hospitality and support during the programme on *Quantum Paths*. This work was supported by the EPSRC under grant EP/N01930X and YDvN is supported by the Merton College Buckee Scholarship and the VSB and Muller Foundations.

Appendix A: Initial states

In this Appendix we construct a class of initial states in which a Wick's theorem holds. Let b_j be the annihilation operators in the mode expansion of the Bose field and consider canonical transformations of the form

$$b_j = A_{jk}a_k + B_{kj}a_k^\dagger + v_j , \quad (\text{A1})$$

where $[a_k, a_k^\dagger] = \delta_{j,k}$ and

$$a_j|i\rangle = 0. \quad (\text{A2})$$

For the transformation to be canonical we require

$$AB = (AB)^T, \quad AA^\dagger - (B^\dagger B)^T = \mathbf{1}. \quad (\text{A3})$$

By construction we have a Wick's theorem in the state $|i\rangle$ and the relevant one and two-point functions are

$$\begin{aligned} \langle i|b_j|i\rangle &= v_j, \\ \langle i|b_k b_p|i\rangle - \langle i|b_k|i\rangle \langle i|b_p|i\rangle &= (AB)_{kp}, \\ \langle i|b_k b_p^\dagger|i\rangle - \langle i|b_k|i\rangle \langle i|b_p^\dagger|i\rangle &= (AA^\dagger)_{kp}. \end{aligned} \quad (\text{A4})$$

Appendix B: Joint Distribution Functions for the phase operator

The goal of this Appendix is to compute full distribution functions for the real and imaginary parts of the following operator

$$\hat{\mathcal{O}}_\ell = \int_{-\ell/2}^{\ell/2} dx e^{i\hat{\phi}(x,t)}, \quad (\text{B1})$$

where the time evolution is calculated in the SCDTHA. The real and imaginary parts of $\hat{\mathcal{O}}_\ell$ are Hermitian and their respective measurement outcomes can be described by a joint PDF $F_\ell(t, a, b)$, which gives the probability density of simultaneously measuring the eigenvalue a for $\text{Re}(\hat{\mathcal{O}}_\ell)$ and the eigenvalue b for $\text{Im}(\hat{\mathcal{O}}_\ell)$ at time t . Once the joint PDF is known, expectation values of analytic functions $g(\text{Re}(\hat{\mathcal{O}}_\ell), \text{Im}(\hat{\mathcal{O}}_\ell))$ can be computed via

$$\left\langle g\left(\text{Re}(\hat{\mathcal{O}}_\ell), \text{Im}(\hat{\mathcal{O}}_\ell)\right) \right\rangle_t = \iint da db F_\ell(t, a, b) g(a, b). \quad (\text{B2})$$

Expanding the approach of Ref. 28, this Appendix presents a computation of the PDF $F_\ell(t, a, b)$, by determining the generic $(m, n)^{\text{th}}$ moment $\langle (\text{Re}(\hat{\mathcal{O}}_\ell))^m (\text{Im}(\hat{\mathcal{O}}_\ell))^n \rangle$, and comparing it to the definition

$$M_{mn}(\ell, t) = \left\langle \left(\text{Re}(\hat{\mathcal{O}}_\ell)\right)^m \left(\text{Im}(\hat{\mathcal{O}}_\ell)\right)^n \right\rangle_t = \iint da db F_\ell(t, a, b) a^m b^n, \quad (\text{B3})$$

from which $F_\ell(t, a, b)$ is then extracted. Expanding sines and cosines in terms of complex exponentials we have

$$M_{mn}(\ell, t) = \left(\frac{1}{2}\right)^m \left(\frac{1}{2i}\right)^n \sum_{\{s_j=\pm 1\}} \left(\prod_{j=m+1}^{m+n} s_j \right) \left(\prod_{k=1}^{m+n} \int_{-l/2}^{l/2} dx_k \right) \left\langle \prod_{l=1}^{m+n} e^{is_l \phi_a(x_l, t)} \right\rangle. \quad (\text{B4})$$

We recall that the mode expansion (34) for the time evolved Bose field has the form

$$\phi(x, t) = \langle \phi(0, t) \rangle + \sum_j u_j e^{iq_j x} \left(Q_j(t) a_j - Q_{-j}^*(t) a_{-j}^\dagger \right), \quad (\text{B5})$$

where a_j annihilate the initial state and with $\langle \phi(0, t) \rangle$ given by (36). To proceed we define functions

$$w_k(\mathbf{x}) = \sum_{j=1}^{m+n} s_j u_k e^{iq_k x_j}. \quad (\text{B6})$$

The expectation value (B4) in the initial state can be expressed in the form

$$\left\langle \prod_{j=1}^{m+n} e^{is_j \phi_a(x_j, t)} \right\rangle = e^{i \sum_{j=1} s_j \langle \phi(0, t) \rangle} \left\langle e^{i \sum_j w_j(\mathbf{x}) (Q_j(t) a_j - Q_{-j}^*(t) a_{-j}^\dagger)} \right\rangle \quad (\text{B7})$$

$$= e^{i \sum_{j=1} s_j \langle \phi(0, t) \rangle} e^{-\frac{1}{2} \sum_j w_j(\mathbf{x}) w_j^*(\mathbf{x}) |Q_j(t)|^2}. \quad (\text{B8})$$

The first exponent on the right-hand side of (B8) contains products of expressions involving different coordinates x_i and x_j with $i \neq j$. This means that the integrals in (B4) over the coordinates x_j cannot be separately carried out. We therefore perform a Hubbard-Stratonovich transformation based on the identity

$$e^{-\frac{q}{2} u^2} = \frac{1}{\sqrt{2\pi q}} \int dz e^{-\frac{1}{2q} z^2} e^{-izu}. \quad (\text{B9})$$

This gives

$$e^{-\frac{1}{2}\sum_j w_j(\mathbf{x})w_j^*(\mathbf{x})|Q_j(t)|^2} = \int_{-\infty}^{\infty} d\alpha_j \int_{-\infty}^{\infty} d\beta_j \frac{e^{-\frac{1}{2}|Q_j(t)|^{-2}(\alpha_j^2+\beta_j^2)}}{2\pi|Q_j(t)|^2} e^{-i\alpha_j \text{Re}w_j(\mathbf{x}) - i\beta_j \text{Im}w_j(\mathbf{x})}. \quad (\text{B10})$$

Substituting (B8), (B10) into (B4), we obtain

$$\begin{aligned} M_{mn}(\ell, t) &= \left(\frac{1}{2}\right)^m \left(\frac{1}{2i}\right)^n \sum_{\{s_l\}} \left(\prod_{l=m+1}^{m+n} s_l\right) \int_{-\infty}^{\infty} d\boldsymbol{\alpha} d\boldsymbol{\beta} \int_{-\ell/2}^{\ell/2} dx \prod_j \frac{e^{-\frac{1}{2}|Q_j(t)|^{-2}(\alpha_j^2+\beta_j^2)} e^{is_j \langle \phi(0,t) \rangle}}{2\pi|Q_j(t)|^2} \\ &\quad \times \exp\left(-i \sum_k (\alpha_k \text{Re}w_k(\mathbf{x}) + \beta_k \text{Im}w_k(\mathbf{x}))\right). \end{aligned} \quad (\text{B11})$$

Reinserting the vector $w_k(\mathbf{x})$ from Eq. (B6) and bringing the sum over signs s_l within the product, this simplifies to

$$\begin{aligned} M_{mn}(\ell, t) &= \int_{-\infty}^{\infty} d\boldsymbol{\alpha} d\boldsymbol{\beta} \prod_j \frac{e^{-\frac{1}{2}|Q_j(t)|^{-2}(\alpha_j^2+\beta_j^2)}}{2\pi|Q_j(t)|^2} \\ &\quad \times \left(\int_{-\ell/2}^{\ell/2} dx \cos(\Phi(x, t, \boldsymbol{\alpha}, \boldsymbol{\beta}))\right)^m \left(\int_{-\ell/2}^{\ell/2} dx \sin(\Phi(x, t, \boldsymbol{\alpha}, \boldsymbol{\beta}))\right)^n, \end{aligned} \quad (\text{B12})$$

where we have defined

$$\Phi(x, t, \boldsymbol{\alpha}, \boldsymbol{\beta}) = \langle \phi(0, t) \rangle - \sum_j |u_j| (\alpha_j \cos(p_j x) + \beta_j \sin(p_j x)). \quad (\text{B13})$$

Comparing (B12) to the definition of the joint PDF in (B3) gives the desired expression for the joint PDF

$$F_\ell(t, a, b) = \int_{-\infty}^{\infty} d\boldsymbol{\alpha} d\boldsymbol{\beta} \prod_j \frac{e^{-\frac{1}{2}|Q_j(t)|^{-2}(\alpha_j^2+\beta_j^2)}}{2\pi|Q_j(t)|^2} \quad (\text{B14})$$

$$\times \delta\left(a - \int_{-\ell/2}^{\ell/2} dx \cos(\Phi(x, t, \boldsymbol{\alpha}, \boldsymbol{\beta}))\right) \delta\left(b - \int_{-\ell/2}^{\ell/2} dx \sin(\Phi(x, t, \boldsymbol{\alpha}, \boldsymbol{\beta}))\right). \quad (\text{B15})$$

By integrating out the variables a or b in this final expression, PDF's of the imaginary and real parts of $\hat{\mathcal{O}}_\ell$ can be obtained, respectively. Furthermore, the two-point function (42) immediately follows from Eq. (B8) by replacing the vector $w_j(\mathbf{x})$ in Eq. (B6) by $\tilde{w}_j(x) = u_j(\sigma e^{iq_j x} + \tau)$.

Appendix C: Further plots for the zero mode

We here present some additional plots for the zero mode, as governed by the quantum mechanics problem described in Sec. IV A. In particular, we show that the weak damping observed in Fig. 2 is not the only behavior found in the framework of the SCTDHA. A change in the initial conditions can cause the oscillation amplitude to increase, rather than decrease, as shown in Fig. 9. This widening of the envelope is particularly pronounced in the SCTDHA result. The exact solution soon reverts to weakly damped behavior, though the time scale for this damping is much longer than that observed in Ref. 31.

¹ Görilitz A, Vogels J M, Leanhardt A E, Raman C, Gustavson T L, Abo-Shaeer J R, Chikkatur A P, Gupta S, Inouye S, Rosenband T and Ketterle W 2001 *Phys. Rev. Lett.* **87**(13) 130402

² Greiner M, Bloch I, Mandel O, Hänsch T and Esslinger T 2001 *Appl. Phys. B* **73** 769

³ Kinoshita T, Wenger T and Weiss D S 2004 *Science* **305** 1125

⁴ Polkovnikov A, Sengupta K, Silva A and Vengalattore M 2011 *Rev. Mod. Phys.* **83**(3) 863

⁵ Essler F H L and Fagotti M 2016 *J. Stat. Mech.* **064002**

⁶ Gogolin C and Eisert J 2016 *Rep. Prog. Phys.* **79** 056001

⁷ Vidmar L and Rigol M 2016 *J. Stat. Mech.* **064007**

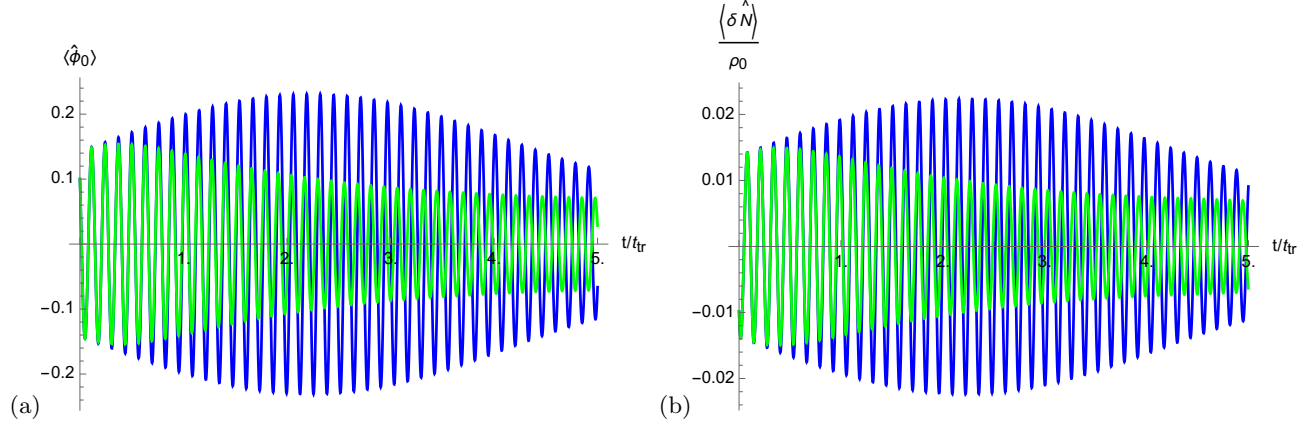


FIG. 9. Comparison between time evolution with H_J (green, Eq. (57)) and the SCTDHA via H'_J (blue, Eq. (59)). Both the zero mode of the phase (a) and its conjugate variable (b) are displayed. All parameters, including the time scale, are as in Fig. 2(b), except that the sign of the initial value δN_0 is reversed.

- ⁸ D'Alessio L, Kafri Y, Polkovnikov A and Rigol M 2016 *Adv. Phys.* **65** 239
- ⁹ Calabrese P and Cardy J 2016 *J. Stat. Mech.* **064003**
- ¹⁰ Calabrese P 2018 *Phys. A: Stat. Mech. Appl.* **504** 31
- ¹¹ Trotzky S, Chen Y A, Flesch A, McCulloch I P, Schollwöck U, Eisert J and Bloch I 2012 *Nature Physics* **8** 325
- ¹² Cheneau M, Barmettler P, Poletti D, Endres M, Schauß P, Fukuhara T, Gross C, Bloch I, Kollath C and Kuhr S 2012 *Nature* **481** 484
- ¹³ Gring M, Kuhnert M, Langen T, Kitagawa T, Rauer B, Schreitl M, Mazets I, Smith D A, Demler E and Schmiedmayer J 2012 *Science* **337** 1318
- ¹⁴ Langen T, Geiger R, Kuhnert M, Rauer B and Schmiedmayer J 2013 *Nat Phys* **9** 640
- ¹⁵ Langen T, Erne S, Geiger R, Rauer B, Schweigler T, Kuhnert M, Rohringer W, Mazets I E, Gasenzer T and Schmiedmayer J 2015 *Science* **348** 207
- ¹⁶ Kaufman A M, Tai M E, Lukin A, Rispoli M, Schittko R, Preiss P M and Greiner M 2016 *Science* **353** 794
- ¹⁷ Andrews M R, Townsend C G, Miesner H J, Durfee D S, Kurn D M and Ketterle W 1997 *Science* **275** 637
- ¹⁸ Schumm T, Hofferberth S, Andersson L M, Wildermuth S, Groth S, Bar-Joseph I, Schmiedmayer J and Kruger P 2005 *Nat Phys* **1** 57
- ¹⁹ Albiez M, Gati R, Fölling J, Hunsmann S, Cristiani M and Oberthaler M K 2005 *Phys. Rev. Lett.* **95**(1) 010402
- ²⁰ Gati R, Albiez M, Fölling J, Hemmerling B and Oberthaler M 2006 *Appl. Phys. B* **82** 207
- ²¹ Levy S, Lahoud E, Shomroni I and Steinhauer J 2007 *Nature* **449** 579
- ²² Hofferberth S, Lesanovsky I, Fischer B, Schumm T and Schmiedmayer J 2007 *Nature* **449** 324–327
- ²³ Kuhnert M, Geiger R, Langen T, Gring M, Rauer B, Kitagawa T, Demler E, Adu Smith D and Schmiedmayer J 2013 *Phys. Rev. Lett.* **110**(9) 090405
- ²⁴ Haldane F D M 1981 *Phys. Rev. Lett.* **47**(25) 1840–1843
- ²⁵ Bistritzer R and Altman E 2007 *Proc. Nat. Acad. Sci.* **104** 9955–9959
- ²⁶ Imambekov A, Gritsev V and Demler E 2007 *eprint arXiv:cond-mat/0703766* (*Preprint cond-mat/0703766*)
- ²⁷ Kitagawa T, Pielawa S, Imambekov A, Schmiedmayer J, Gritsev V and Demler E 2010 *Phys. Rev. Lett.* **104**(25) 255302
- ²⁸ Kitagawa T, Imambekov A, Schmiedmayer J and Demler E 2011 *New J. Phys.* **13** 073018
- ²⁹ Gritsev V, Polkovnikov A and Demler E 2007 *Phys. Rev. B* **75**(17) 174511
- ³⁰ Schweigler T, Kasper V, Erne S, Mazets I, Rauer B, Cataldini F, Langen T, Gasenzer T, Berges J and Schmiedmayer J 2017 *Nature* **545** 323
- ³¹ Pigeur M, Berrada T, Bonneau M, Schumm T, Demler E and Schmiedmayer J 2018 *Phys. Rev. Lett.* **120**(17) 173601
- ³² Pigeur M and Schmiedmayer J 2018 *arXiv e-prints* arXiv:1810.02772 (*Preprint 1810.02772*)
- ³³ Dalla Torre E G, Demler E and Polkovnikov A 2013 *Phys. Rev. Lett.* **110**(9) 090404
- ³⁴ Iucci A and Cazalilla M A 2009 *Phys. Rev. A* **80** 063619
- ³⁵ Iucci A and Cazalilla M A 2010 *New J. Phys.* **12** 055019
- ³⁶ Foini L and Giamarchi T 2015 *Phys. Rev. A* **91**(2) 023627
- ³⁷ Foini L and Giamarchi T 2017 *Eur. Phys. J. Spec. Top.* **226** 2763–2774
- ³⁸ Bertini B, Schuricht D and Essler F H L 2014 *J. Stat. Mech.* **P10035**
- ³⁹ Caux J S and Essler F H L 2013 *Phys. Rev. Lett.* **110**(25) 257203
- ⁴⁰ Caux J S 2016 *J. Stat. Mech.* **064006**
- ⁴¹ Calabrese P, Essler F H L and Fagotti M 2012 *J. Stat. Mech.* **P07016**
- ⁴² Schuricht D and Essler F H L 2012 *J. Stat. Mech.* **P04017**
- ⁴³ Kormos M and Zaránd G 2016 *Phys. Rev. E* **93** 062101
- ⁴⁴ Sachdev S and Young A P 1997 *Phys. Rev. Lett.* **78** 2220
- ⁴⁵ Iglói F and Rieger H 2011 *Phys. Rev. Lett.* **106**(3) 035701

- ⁴⁶ Cubero A C and Schuricht D 2017 *J. Stat. Mech.* **103106**
- ⁴⁷ James A J A, Konik R M, Lecheminant P, Robinson N J and Tsvelik A M 2018 *Rep. Prog. Phys.* **81** 046002
- ⁴⁸ Horváth D and Takcs G 2017 *Phys. Lett. B* **771** 539
- ⁴⁹ Horváth D X, Kormos M and Takács G 2018 *J. High Energ. Phys.* **170**
- ⁵⁰ Moca C, Kormos M and Zaránd G 2017 *Phys. Rev. Lett.* **119**(10) 100603
- ⁵¹ Kukuljan I, Sotiriadis S and Takacs G 2018 *Phys. Rev. Lett.* **121**(11) 110402
- ⁵² Horvath D X, Lovas I, Kormos M, Takacs G and Zarand G 2018 *ArXiv e-prints* (*Preprint* 1809.06789)
- ⁵³ Chang S J 1975 *Phys. Rev. D* **12**(4) 1071–1088
- ⁵⁴ Sotiriadis S and Cardy J 2010 *Phys. Rev. B* **81** 134305 (*Preprint* 1002.0167)
- ⁵⁵ Boyanovsky D, Cooper F, de Vega H J and Sodano P 1998 *Phys. Rev. D* **58**(2) 025007
- ⁵⁶ Bertini B, Essler F H L, Groha S and Robinson N J 2015 *Phys. Rev. Lett.* **115**(18) 180601
- ⁵⁷ Bertini B, Essler F H L, Groha S and Robinson N J 2016 *Phys. Rev. B* **94**(24) 245117
- ⁵⁸ van Nieuwkerk Y D and Essler F H L *In preparation*
- ⁵⁹ Smith D A, Gring M, Langen T, Kuhnert M, Rauer B, Geiger R, Kitagawa T, Mazets I, Demler E and Schmiedmayer J 2013 *New J. Phys.* **15** 075011
- ⁶⁰ Cherng R W and Demler E 2007 *New J. Phys.* **9** 7
- ⁶¹ Lamacraft A and Fendley P 2008 *Phys. Rev. Lett.* **100**(16) 165706
- ⁶² Ivanov D A and Abanov A G 2013 *Phys. Rev. E* **87**(2) 022114
- ⁶³ Shi Y and Klich I 2013 *J. Stat. Mech.* **P05001**
- ⁶⁴ Eisler V 2013 *Phys. Rev. Lett.* **111**(8) 080402
- ⁶⁵ Klich I 2014 *J. Stat. Mech.* **P11006**
- ⁶⁶ Stéphan J M and Pollmann F 2017 *Phys. Rev. B* **95**(3) 035119
- ⁶⁷ Moreno-Cardoner M, Sherson J F and De Chiara G 2016 *New J. Phys.* **18** 103015
- ⁶⁸ Collura M, Essler F H L and Groha S 2017 *J. Phys. A: Math. Theor.* **50** 414002
- ⁶⁹ Najafi K and Rajabpour M A 2017 *Phys. Rev. B* **96**(23) 235109
- ⁷⁰ Lovas I, Dóra B, Demler E and Zaránd G 2017 *Phys. Rev. A* **95**(5) 053621
- ⁷¹ van Nieuwkerk Y D, Schmiedmayer J and Essler F H L 2018 *SciPost Phys.* **5**(5) 46
- ⁷² Bastianello A, Piroli L and Calabrese P 2018 *Phys. Rev. Lett.* **120**(19) 190601
- ⁷³ Groha S, Essler F H L and Calabrese P 2018 *SciPost Phys.* **4** 43
- ⁷⁴ Bastianello A and Piroli L 2018 *J. Stat. Mech.* **113104**
- ⁷⁵ Sakaguchi T, Tamaribuchi T and Takada S 1982 *Progr. Theor. Phys.* **68** 19
- ⁷⁶ Essler F H and Konik R M 2005 *Applications of Massive Integrable Quantum Field Theories to Problems in Condensed Matter Physics* (World Scientific) pp 684–830
- ⁷⁷ Zamolodchikov A B 1995 *Int. J. Mod. Phys. A* **10** 1125
- ⁷⁸ Cazalilla M A 2004 *J. Phys. B* **37** S1